

Bolted end plate connections for steel reinforced concrete composite structures

Xian Li¹, Yuntian Wu², Weifeng Mao¹, Yan Xiao^{1,2†},
J. C. Anderson² and Yurong Guo¹

¹College of Civil Engineering, CIPRES, Hunan University, Changsha, China

²Department of Civil Engineering, University of Southern California, Los Angeles, USA

(Received August 29, 2005, Accepted March 28, 2006)

Abstract. In order to improve the constructability and meanwhile ensure excellent seismic behavior, several innovative composite connection details were conceived and studied by the authors. This paper reports experimental results and observations on seismic behavior of steel beam bolted to reinforced concrete column connections (bolted RCS or BRCS). The proposed composite connection details involve post tensioning the end plates of the steel beams to the reinforced concrete or precast concrete columns using high-strength steel rods. A rational design procedure was proposed to assure a ductile behavior of the composite structure. Strut-and-tie model analysis indicates that a bolted composite connection has a favorable stress transfer mechanism. The excellent capacity and behavior were then validated through five full-scale beam to column connection model tests.

Keywords: beam-column connection; bolted end plate; hybrid structure; reinforced concrete column; steel beam; seismic design.

1. Introduction

One of the most significant lessons learned from the 1994 Northridge earthquake and the 1995 Kobe earthquake was the cracking and brittle failure of welded moment connections of modern steel buildings (Bertero *et al.* 1994, 1995). Several important progresses have since been made, resulting in improved designs (Anderson *et al.* 2001, SAC FEMA 350, Xiao and Mahin 2000 edited).

A possible solution for improving the design and construction of moment resisting frame (MRF) buildings ranging in height from mid-rise to high-rise may be the adoption of composite steel and concrete MRF systems in the regions of high seismicity. Because of the existence of reinforced concrete and the high stiffness in a composite MRF, the deformation demand to the encased steel joints becomes less than in a pure steel MRF. Smoother force transferring mechanisms with less stress concentration can be expected in a composite beam-to-column connection. Thus, at least the development of composite MRFs can provide the structural design and construction professions with an alternative structural system.

† Associate Professor, Corresponding author, E-mail: yanxiao@usc.edu

In general, composite steel and concrete structures have the following advantages compared with steel structures:

- i. By encasing steel shapes in reinforced concrete or using concrete filled tubular columns, a composite system can provide high lateral stiffness which is important for tall buildings.
- ii. Anti-buckling behavior of steel shapes can be significantly improved.
- iii. Composite structures or structural members have relatively high rigidity and damping against vibration, and thus are especially desirable for residential, hotel and office buildings. The concrete finishing is also favored architecturally.
- iv. The combination with concrete not only provides the above mechanical merits, but can also greatly improve fire resistance.

On the other hand, composite steel and concrete structures have the following advantages compared with reinforced concrete (RC) structures:

- i. Properly designed composite steel and concrete members can prevent the brittle failure mode of reinforced concrete members and have significant ductility.
- ii. The size of the members can be made smaller thus increasing strength/weight ratios.
- iii. The encased steel frame can be used as shoring system for concrete forms during construction.

In the United States, most of the previous research on composite frames has been focused on reinforced concrete steel (RCS) connections between reinforced concrete columns and steel beams (ASCE Task 1994, Deierlein *et al.* 1989, Griffis 1986, Leon *et al.* 1996, Sheikh *et al.* 1989). In a typical RCS system, a small steel section is encased in the column primarily for erection purposes rather than for transferring forces. Research carried out by others (Peng *et al.* 2000) has indicated that innovative details using post-tensioning and bolting can provide adequate strengths and ductility for steel or concrete filled tubular (CFT) MRF structures. Only limited research has been performed to evaluate the seismic performance of SRC connections that consist of steel-encased reinforced concrete (SRC) column and steel beam (Chou and Uang 1998, 2000). Uang and Chou tested two full-scale subassemblies with SRC columns and steel beams to evaluate the seismic performance of the connection details (Chou and Uang 1998, 2000). Promising seismic behavior has been observed in their research for connections with reduced steel beam section as well as using offset doubler plates. However, the details investigated by Uang *et al.* were still quite complicated with the requirement of a welded steel beam to column connection.

2. Proposed SRC-MRF connections

In order to improve the constructability and meanwhile ensure excellent seismic behavior, several innovative composite connection details were conceived by Xiao *et al.* (2003). The new type of composite steel and concrete moment resisting frame system adopts bolted end plate connections without the need of field welding. This paper discusses the test results for one of the proposed connections.

As shown in Fig. 1, this type of connection has a detail with directly connecting the end plate of the steel beam to the column by post-tensioning. This creates more freedoms for the design, as the columns can be SRC, RC, and particularly suitable for precast (PC) construction of the columns. Fig. 1 schematically depicts a connection with steel beam post-tensioned to a PC column. Study of steel beam and PC column connection is the main subject of this paper.

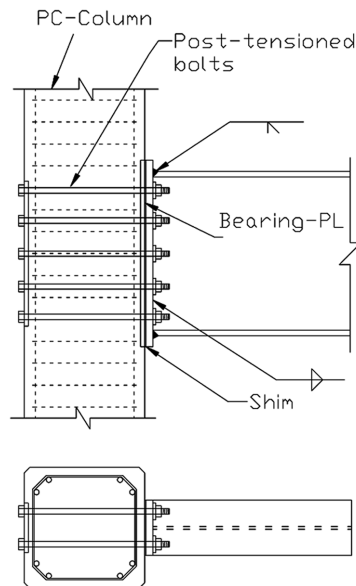


Fig. 1 Proposed BRCS beam column connection

The connection proposed herein is different compared with Peng *et al.*'s post-tensioned connections (Peng *et al.* 2000, Rojas *et al.* 2002) where the post-tensioning is for the entire length of the steel beams in a floor. Previous research on joints between reinforced concrete walls and steel coupling beams provides useful references to this study in terms of how to design the details of the connection (Shahrooz *et al.* 2000, Shen and Kurama 2000).

3. Suggested design approach

One of the objectives of the connection design is to assure the ductile failure pattern of the connection. A capacity design approach was proposed and followed in the selection of the specimens. The approach includes the following steps:

- i. To choose a mechanism where plastic hinges occurring at the ends of the steel beams and at the base of the first floor columns;
- ii. Design concrete or steel-concrete composite columns for sufficient flexural and shear strength and ductility to ensure the mechanism;
- iii. Design the end plates and selection of post-tensioning bolts;

Beam-column joint shear check following two criteria: (1) joint shear cracking check by comparing the principal tensile stress with the concrete tensile strength; (2) if joint shear cracking is identified in (1), then conduct strut-and-tie analysis to determine the shear reinforcement.

4. Steel beam bolted to RC column connections

Five full-scale steel beam bolted to RC column exterior connection specimens were designed and

tested. Table 1 shows the details of the four specimens. Material properties of specimens are summarized in Table 2. In order to take full advantages of existing data and testing experiences at the laboratory, the welded steel beam section was made to closely represent AISC W24 × 76 steel section. Selection of this steel shape allowed to compare the test results of the current project with those conducted for welded SRC column and steel beam connections by Chou and Uang (1998, 2000) and the welded steel connections tested by the authors (Anderson *et al.* 2002). Based on the proposed design procedure and considering the dimensions of Uang's specimens, the basic details of

Table 1 Model specimen details

Specimen		BRCS-EJ1	BRCS-EJ2	BRCS-EJ3	BRCS-EJ4	BRCS-EJ5
Steel beam	Section (mm) ($h \times b \times t_f \times t_w$)	606 × 230 × 16 × 12				
	Length* (mm)	2850	2850	2710	2410	2410
	Reduced beam end	N/A	N/A	Dog-bone	Dog-bone	Dog-bone
End plate	Dimension (mm) ($h \times b \times t$)	810 × 305 × 35	810 × 305 × 40	810 × 305 × 40	946 × 480 × 40	946 × 480 × 40
High-strength bolt	Nominal diameter (mm)	22	24	24	30	30
	Number of rows	7	7	7	4	4
	Number per row	2	2	2	4	4
RC column	Height (mm)	3800	3800	3800	3800	3800
	Section width (mm) × depth (mm)	560 × 560	560 × 560	560 × 560	540 × 540	540 × 540
	Longitudinal bar	HRB400Φ25	HRB400Φ25	HRB400Φ25	HRB400Φ25	HRB400Φ25
	Longitudinal steel ratio	2.5%	2.5%	2.5%	2.7%	2.7%
	Transverse bar	HRB400Φ14	HRB400Φ14	HRB400Φ14	HPB235Φ12	HPB235Φ12
	Concrete strength** (MPa)	39.4	41.4	41.4	40.1	46.1

Note: * beam length includes end plate thickness; ** concrete strength is taken as 80% of the compressive strength based on cubic specimens.

Table 2 Steel properties

Category	Call names	Yield strength f_y (MPa)	Ultimate strength f_u (MPa)	Elastic modulus E_c (MPa)
RC column longitudinal bar	HRB400Φ28	412	555	2.09×10^5
	HRB400Φ25	458	642	2.07×10^5
RC column transverse bar	HRB400Φ14	485	713	2.04×10^5
	HPB235Φ12	338	507	2.12×10^5
Steel flange	$t_f = 16$ mm	369.8	447.5	2.09×10^5
Steel web	$t_w = 12$ mm	387.5	468.9	2.08×10^5
Bolt	M22	959	1128	–
	M24	924	1101	–
	M30	893	1026	–

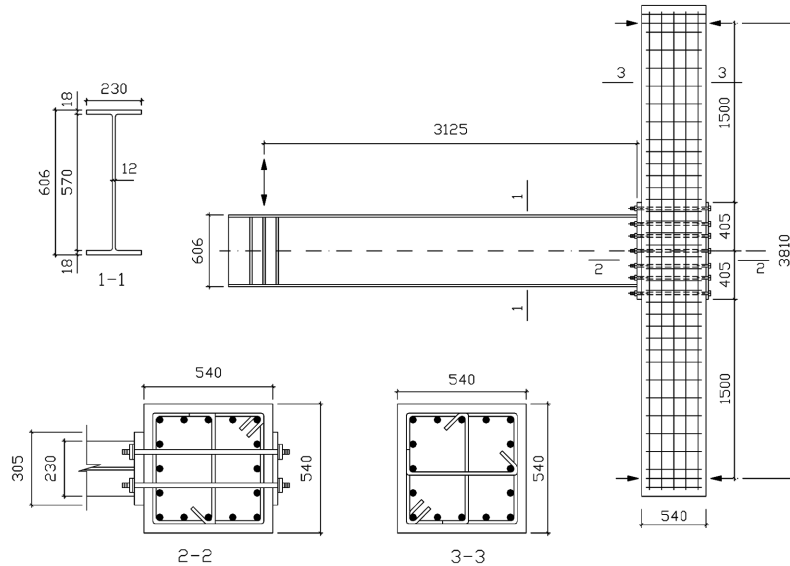


Fig. 2 Specimen details

exterior connection models were chosen and shown in Fig. 2. The design and analysis of the specimens are described hereafter. Note that the strength reduction factors are taken to be unit for the design of specimens.

4.1 Flexural strength of steel beam

For seismic design, the nominal strength of the steel beam can be calculated as the plastic moment, M_p ,

$$M_p = F_y Z \quad (1)$$

where, F_y is the yield strength of the steel and Z is the plastic section modulus. The corresponding shear V_p in the steel beam with a clear shear span length l_b can then be determined as,

$$V_p = M_p / l_b \quad (2)$$

The AISC W24 × 76 beam has a plastic section modulus $Z = 3.28 \times 10^6 \text{ mm}^3$ (200 in.³). If ASTM A572 Grade 50 Steel (yield strength $F_y = 345 \text{ MPa} = 50 \text{ ksi}$) is used, then the plastic moment is calculated as $M_p = F_y Z = 1130 \text{ kNm}$ (10,000 kip-in.), and the shear force corresponding to the plastic moment is, $V_p = M_p / l_b = 1130 / 3.125 = 361.2 \text{ kN}$. The specimens were made with welded wide-flange sections approximately equal to the AISC W24 × 76. The steel material was the Q345 per the Chinese standards, which was identical to the Grade 50 steel in the US market. For specimen BRCS-EJ3 and EJ4, the width of the steel beam flanges near the critical moment end was reduced to form the so-called dog-bone detail following the recommendations of FEMA 350 (2000).

4.2 Reinforced concrete column design

The shear demands in the columns and the moment demands at column ends can be calculated based on the need to counteract the plastic moment acting at the end of the steel beam. For a story height of 3.4 m, the shear in the columns was calculated as $V_c = 358$ kN, and the moment demand at the beam column interface was then 464 kNm. Based on ACI-318 codes, the reinforcements for the 540×540 mm square column with design concrete strength of $f'_c = 35$ MPa (5.08 ksi) was determined and shown in Fig. 5. The column as reinforced with 16 No. 25 (nominal diameter = 25.4 mm) A706 (nominal yield strength = 420 MPa) bars, constituting a total longitudinal steel ratio of 2.5%.

4.3 End plate

The thickness of the end plate can be estimated based on the so-called tee-stub analogy (AISC 2001). A thickness of 35 mm was chosen for the endplate of the $W24 \times 76$ equivalent steel beam. However, except for the first specimen, 40 mm thick endplates were used for all the specimens for increased stiffness.

4.4 Post-tensioned bolts

Three possible approaches can be considered in the design of the post-tensioned bolts, similar to elastic and ultimate design approaches for prestressed concrete beam. The first method is based on a no-tension criterion, and the resultant of the linearly distributed stresses in the steel end plate and the concrete column interface needs to resist the moment demand, M_p . The second approach is based on a resisting mechanism shown in Fig. 3, where the bolts on the tension side resist tension at their ultimate capacities and the concrete rectangular stress block based on ACI 318 codes provides the compressive resistant. The third method is based on an elastic linear distribution of bolt forces and the ultimate condition is determined when the extreme tensile bolts develop the strength. It is also suggested that the compressive strength of the concrete for the design can be amplified as a bearing strength using $\sqrt{b_c/b_{ep}}$, here b_c and b_{ep} are the widths of the concrete column and the endplate, respectively. The compression zone depth can then be calculated as,

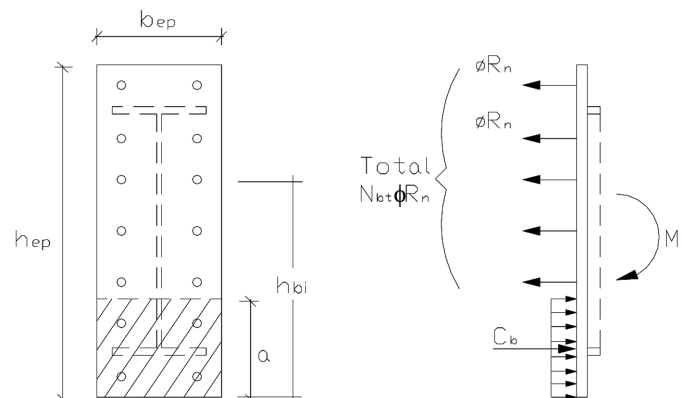


Fig. 3 Ultimate condition at endplate and column interface

$$a = \frac{N_{bt}\phi R_n}{0.85 b_{ep} f'_c \sqrt{b_c / b_{ep}}} \tag{3}$$

where, N_{bt} is the number of the rows of bolts on the tension side; R_n is the nominal capacity of one row of bolts; and ϕ is the strength reduction factor. The strength reduction factor ϕ can be selected according to current design codes or modified for assuring the strong beam and weak column design. The nominal moment capacity, M_{nep} , at the interface of the bearing plate and column can be calculated by taking moment about the center of the compression zone.

$$M_{nep} = \phi R_n \sum (h_{bi} - a/2) \tag{4}$$

where, h_{bi} is the depth of the i -th row of bolts measured from the bottom edge of the endplate.

Fourteen A490 bolts aligned in 7 rows were chosen for first three specimens. The bolt types used for specimens EJ1, EJ2 and EJ3 were selected based on the ultimate design approach while that for EJ4 and EJ5 based on the elastic method.

4.5 Joint shear – cracking check

A conservative design of the beam-column connection is to size the connection zone big enough to eliminate the possibility of joint shear cracking. Similar to the method proposed for column-footing connection (Xiao *et al.* 1996), principal tensile stress can be calculated and compared with the tensile strength of concrete. As shown in Fig. 4(a), the tensile and compressive resultants and shear forces at each of the beam-column interface sections can be analyzed for the ultimate loading condition corresponding to M_p . Note the special feature of the proposed bolted connection where the tension force in at the beam end $N_{bt}\phi R_n$ is transmitted to the other side of the beam-column connection. Applying these forces on the boundary of the connection zone, the average normal and shear stresses in the horizontal and vertical sections, shown in Figs. 4(b) and (c), can be estimated as follows,

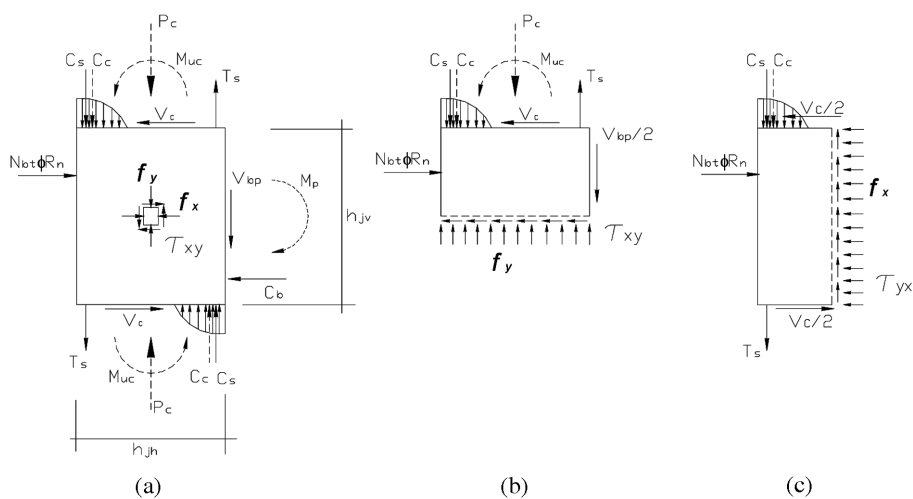


Fig. 4 Joint shear stresses

$$f_x = \frac{N_{bt}\phi R_n}{b_j h_{jv}} \tag{5a}$$

$$f_y = \frac{C_c + C_s - T_s}{b_j h_{jh}} \tag{5b}$$

$$\tau_{xy} = \frac{N_{bt}\phi R_n - V_c}{b_j h_{jh}} \tag{5c}$$

$$\tau_{yx} = \frac{C_c + C_s + T_s}{b_j h_{jv}} \tag{5d}$$

where, b_j is the joint width; h_{jh} and h_{jv} are the depths of the horizontal and vertical sections, respectively. For simplicity, b_j and h_{jh} can be taken as the column width and depth, whereas h_{jv} can be taken as the depth of the steel beam. Note that theoretically τ_{xy} and τ_{yx} are the same magnitude. If they are calculated with different values due to different assumptions for the horizontal and vertical sections, the larger value should be used. The principal tensile stress can then be calculated based on the subtraction operation of the following equations,

$$p_t^c = \left(\frac{f_x + f_y}{2} \right) \pm \sqrt{\left(\frac{f_x - f_y}{2} \right)^2 + \tau^2} \tag{6}$$

If the calculated principal tensile stress p_t exceeds $0.29\sqrt{f'_c}$ (Priestley *et al.* 1996), cracking is expected in the connection and additional reinforcement is needed for the shear resistance in the joint region. For the exterior connection specimen in this study, the principal tensile stress was calculated as 4.5 MPa > $0.29\sqrt{f'_c} = 1.7$ MPa. It was deemed impractical and inefficient design to further enlarge the column size, thus further analysis for a cracked connection was necessary.

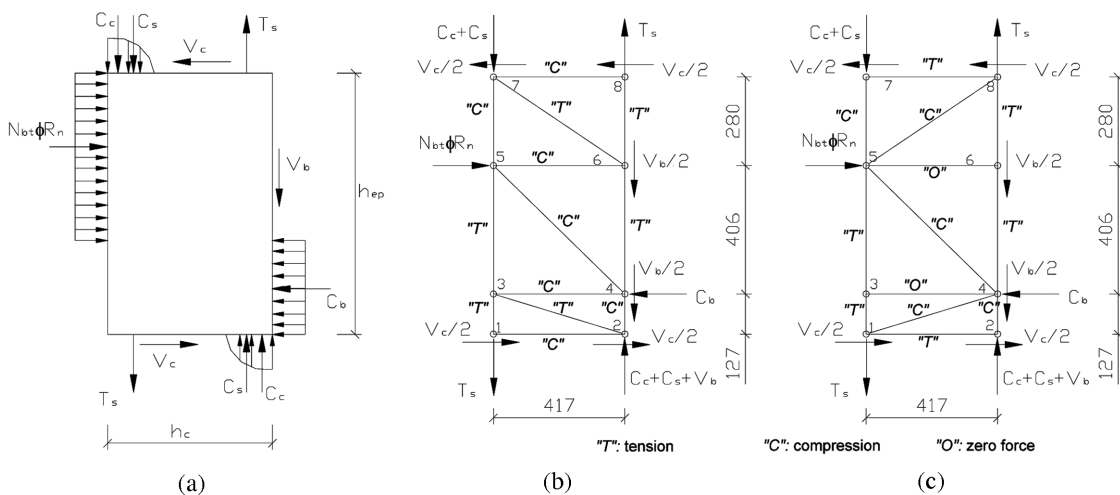


Fig. 5 Strut-and-tie models

4.6 Joint shear – strut-and-tie model

The resulting forces corresponding to the ultimate condition are applied on the boundary of the connection zone with the dimension of the column section and the height of the endplate, as shown in Fig. 5(a). By combining the compressive forces provided by the concrete and compressive steel bars in the column sections and assuming nodes at the intersections of the application lines of various resulting forces, the first simple strut-and-tie model can be constructed as illustrated in Fig. 5(b).

For the given conditions, the forces in the elements of the model are analyzed and marked for tension by “T”, compression by “C” and zero element by “0”, in Fig. 5(b). It is interesting to note that all the horizontal elements which suppose to be ties for a conventional joint are identified to be subjected to compressive forces, while two of the intended struts (struts 2-3 and 6-7) actually become ties, indicating tensile stress fields in those directions. If assuming no tensile force can be carried by the concrete struts, the revised strut-and-tie model shown in Fig. 5(c) should be considered. The analysis of the revised strut-and-tie model indicates that the horizontal joint reinforcements are only needed near the vicinities of the column ends. It is also important to notice that the tensile forces in vertical ties 1-3, 3-5, 4-6 and 6-8 are all larger than the yield forces of the tensile bars. This indicates that additional vertical reinforcements may be needed in the connection region. However, in the testing specimen design, this was not particularly considered because the vertical tie forces only exceeded the yield forces with a small margin.

5. Experimental program

5.1 Test method

The test setup was designed to subject the exterior beam to column connection model to simulated seismic loading conditions, in terms of moment and shear force distributions, as shown in Fig. 6. A 120-ton pseudo-controlled actuator was positioned vertically at the free end of the steel beam to

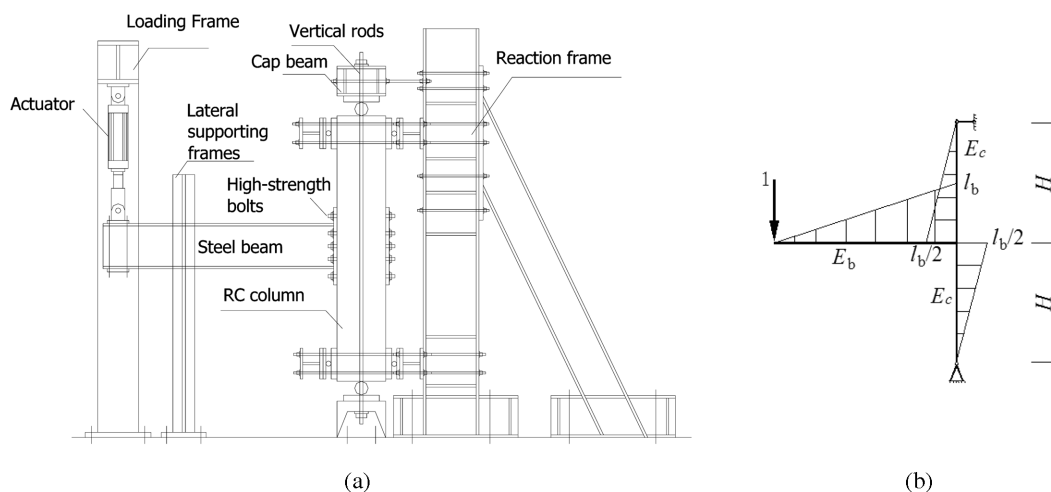


Fig. 6 Loading method; (a) test setup, (b) loading condition

apply cyclic shear force to the beam. The top and the bottom ends of the reinforced concrete column were tied to the strong reaction floor and the reaction frame by cap beams and strong ties. Rollers were provided between the column and the cap beams in the attempt to simulate pinned supports at the column ends. Two specially designed frames were positioned near the free end of the steel beam to prevent the accidental out-of-plane deformation. Ball bearings were provided between the frames and the steel beam to allow the beam end move freely in the vertical direction.

The loading sequence was controlled by the displacement, Δ , at shear force application point near the beam free end, corresponding to the rotational angle, defined as the ratio of the displacement Δ and the length of the beam, L . One cycle each corresponding to an increment of peak rotational angle of $\Delta/L = 0.25\%$, till $\Delta/L = 0.75\%$. Then three complete loading cycles were attempted corresponding to peak rotational angles at $\Delta/L = 1.0\%$, 1.5% , 2% , 3% , 4% , till the model connection failed or developed any major physical changes.

The instrumentation included the displacements at free end of the beam along the line of load application, and several locations along the beam, using linear potensometers. Linear potensometers were also installed in the beam to column connection zone to obtain information related to the joint shear deformation. Electrical resistance strain gauges were affixed on steel bars before concrete casting and on the surfaces of the steel beam at predefined locations.

6. Experimental results on proposed steel beam bolted to RC column connections (BRCS)

6.1 General results

The experimental program was designed to investigate the seismic performance of the proposed type-3 connection details or steel beam bolted to RC column connections. The proposed connection design methods were also examined. The hysteretic loops for three specimens are shown in the Figs. 7(a), 8(a), 9(a) and 10(a), respectively. The corresponding final failure conditions are also shown in these figures.

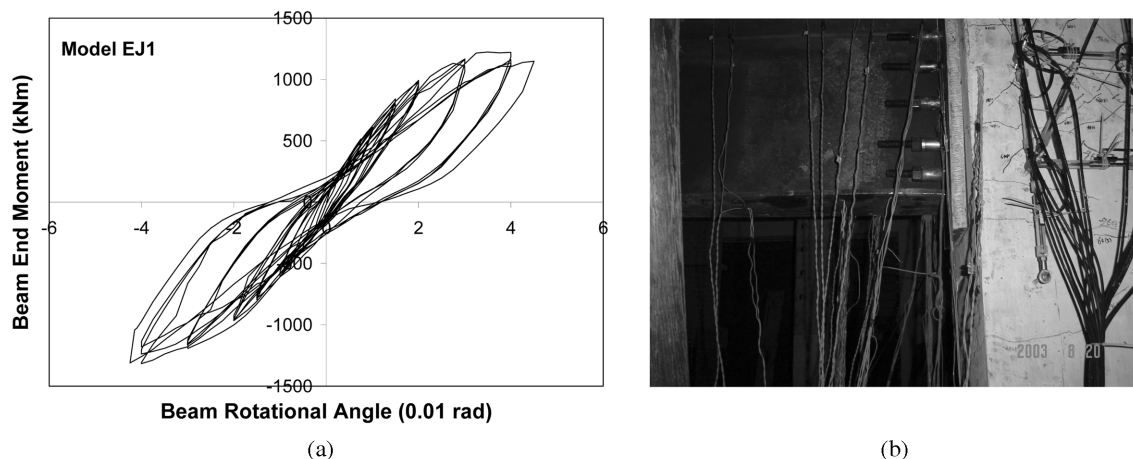


Fig. 7 Test results of specimen BRCS-EJ1; (a) hysteresis loops, (b) rupture of outmost rows of bolts

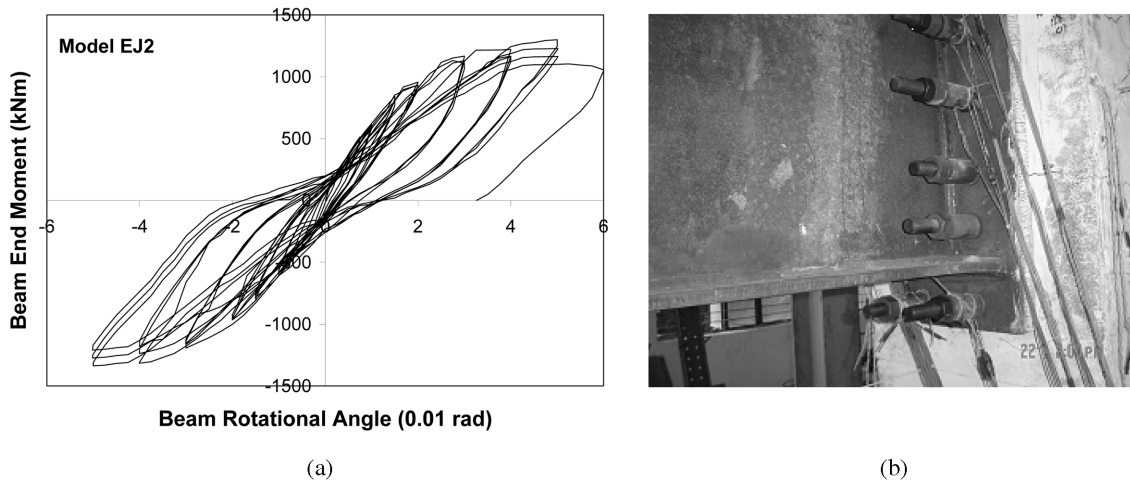


Fig. 8 Test results of specimen BRCS-EJ2; (a) hysteresis loops, (b) yielding of reduced flange width zone and rupture of outermost rows of bolts

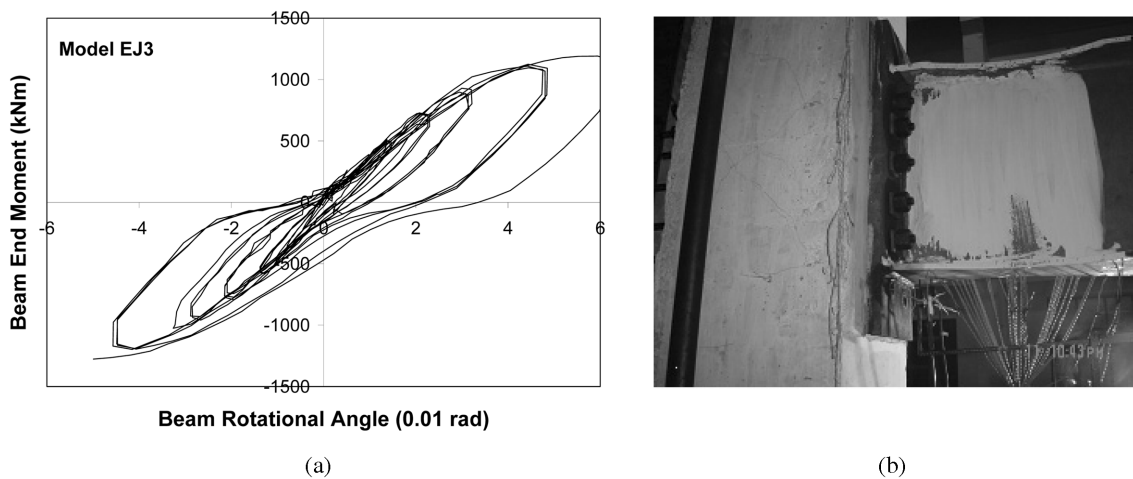


Fig. 9 Test results of specimen BRCS-EJ3; (a) hysteresis loops, (b) rupture of end plate

6.1.1 Models EJ1 and EJ2

For specimen EJ1, one bolt in tension in the outermost row fractured before plastic hinge could fully formed at the beam end. For specimen EJ2, since a thicker end plate and bolts with larger diameters were used, the moment carrying capacity increased correspondingly. When the rotational angle reached 0.03 rad., the endplate was clearly seen separated from the column face in the tension side. The peak load carrying capacity was developed corresponding to the first peak at a rotational angle of 0.05 rad. After this stage, the capacity degraded gradually. The posttest observation indicated that the bolts at the outermost rows became loosely attached due to significant residual deformation. As shown in Figs. 7 and 8, it is interesting to note that the hysteresis loops of the first two models EJ1 and EJ2 are somewhat similar to reinforced concrete beam to column connections characterized by the significant softening of the stiffness prior to reach the peak loading capacity.

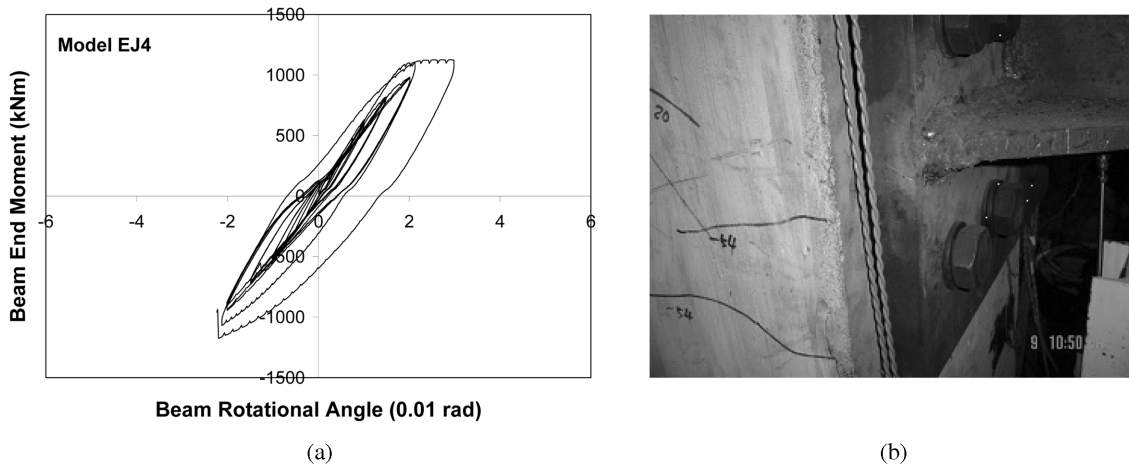


Fig. 10 Test results of specimen BRCS-EJ4; (a) hysteresis loops, (b) rupture of end plate

Although the strain measurements revealed the yielding of the steel beam, a full plastic hinge in the steel beam was not developed.

6.1.2 Model EJ3

The connection model EJ3 was a retest specimen using the RC beam of model EJ2 and the steel beam re-fabricated from the steel beam of EJ1 with the addition of a dog-bone detail. As shown in Fig. 9(a), the hysteretic behavior of EJ3 was similar to those of previous two model connections, however with reduced stiffness due to the fact of using the tested RC column and a steel beam with reduced flange zone. As shown in Fig. 9(b), the steel beam yielded in the reduced flange width zone, as evidenced by the falling of the flakes of the oxidized skins along the whitewash painting. The web was also seen to have started local buckling when the total rotational angle exceeded 0.04 rad. The sudden rupture of a bolt at the lowest row triggered the failure of the specimen during the loading to complete the cycle at a peak rotational angle of 0.06 rad.

6.1.3 Model EJ4 and model EJ5

The model connection specimen EJ4 demonstrated a limited ductility. The specimen failed during the loading to complete the first cycle corresponding to a peak rotational angle of 0.03 rad. due to the fracture of the end plate, as shown in Fig. 10(b). This was due to the loosened quality control while the end plate was welded to the steel beam. No preheating was practiced by the welder despite the low room temperature.

Model connection EJ5 was specimen with replaced steel beam of failed specimen EJ4. The welding of the end plate to the steel beam was made by a higher skill professional welder with controlled speed and heating. As a consequence, the specimen achieved the most satisfactory hysteretic behavior. The specimen was able to develop an overall rotational angle of 0.03 rad. before any degradation, as shown in Fig. 11(a). At the peak total rotational angle of 0.04 rad., the estimated inelastic rotation was estimated as about 0.034 rad., exceeding the required 0.03 rad. for special steel moment resisting frame per AISC (1999). Gradual degradation in the moment carrying capacity was seen in the hysteretic response in the subsequent loading cycles corresponding to

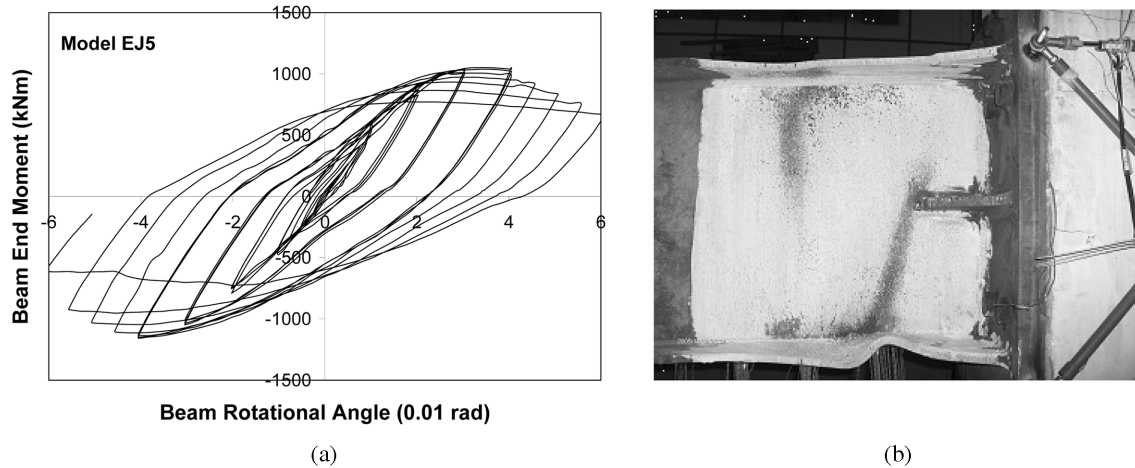


Fig. 11 Test results of specimen BRCS-EJ5; (a) hysteresis loops, (b) plastic hinging of reduced flange width zone at beam end

larger peak rotational angles, as a result of plastic local buckling of the web and flanges in the reduced flange width zone near the beam end, as shown in Fig. 11(b). Throughout the loading, the steel end plate was not separated from the column face.

6.2 Load carrying capacity

Since a safety factor of 1.0 was used in the design of the model connections, the further increase of load carrying capacity corresponding to the strain hardening in the steel beam may have exceeded the capacity that can be offered by the bolts for the first two specimens. In actual design project, an improved connection ductility can be achieved by using a safety factor more than 1.0 or a strength reduction factor less than 1.0. Thus the objective of assuring a ductile failure pattern of the connection can be achieved by using the proposed design approach even with the plastic analysis of the bolts. It is apparent from the test results of models EJ5, satisfactory seismic design can be achieved using the proposed design approach along with an elastic analysis of the high-strength bolts.

6.3 Initial stiffness

The initial stiffness of this new type of connection can be estimated based on the assumption of rigid connection using the elastic stiffness of steel beam and reinforced concrete column. According to the principle of virtual work, the beam tip displacement Δ under the application of the unit force shown in Fig. 6(b) can be determined.

$$\Delta = \frac{l_b}{3} \left(\frac{l_b^2}{E_b I_b} + \frac{H^2}{E_c I_c} \right) \quad (7)$$

Therefore, we can obtain the theoretical relationship between the beam tip force P and beam tip displacement Δ , based on linear elastic analysis As shown in the Fig. 12 for two of the specimens,

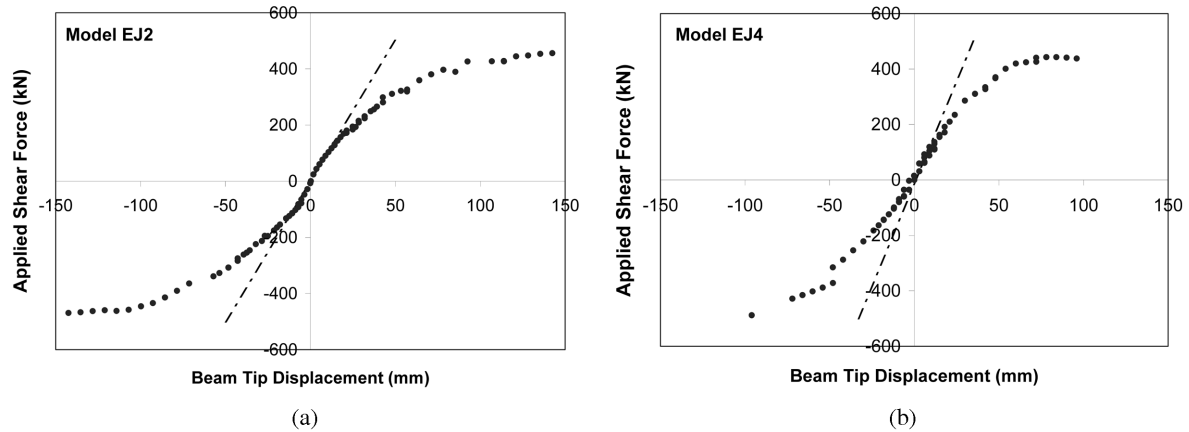


Fig. 12 Comparison of theoretical and experimental initial stiffness for models; (a) EJ2, (b) EJ4

the initial stiffness of the testing models were well predicted by the elastic analysis. Further softening of the stiffness is considered due to the cracking of the reinforced concrete columns and the inelastic deformation of the bolts.

7. Conclusions

New steel and concrete composite moment resisting frame systems are proposed along with several innovative connection details. The proposed connections involve post-tensioning the shop-welded endplates of the steel beams to the concrete, precast and prestressed concrete or steel and concrete columns. There is no field welding, eliminating the problems of the *in-situ* welded steel connections. A rational design approach is also suggested for the design of the elements and the beam-to-column connections.

From the experiment studies on five specimens with the bolted reinforced concrete column and steel beam (BRCS) connection details, the following conclusions can be drawn:

- (i) The proposed connection for the steel beam bolted to RC column composite structures exhibited good ductility and energy-dissipating ability.
- (ii) The proposed design method can result in a ductile failure pattern for the connection, particularly along with the use of the steel beam with the reduced flange width near the critical moment end.
- (iii) The BRCS connections with the high-tension bolts designed based on a plastic analysis developed a hysteretic behavior and failure dominated by the yielding and rupture of the bolts, whereas the behavior was dominated by the inelastic deformation of steel beam when the bolted connection was designed based on an elastic analysis.
- (iv) The initial stiffness of the proposed composite connection can be calculated based on a rigid connection assumption along with the use of the elastic stiffness of steel beam and the reinforced concrete column.

Acknowledgements

The research was conducted as the international collaboration between the University of Southern California of USA and the Hunan University of China. The research was initiated with a project funded by the National Science Foundation under the contract number CMS-0220067. Tests reported in this paper were executed at the Hunan University sponsored by the Cheung Kong Scholarship of the Ministry of Education, the Hunan Construction Bureau, the CIPRES-985 project. The international collaboration was also facilitated by the travel supports of the NSF US-China Cooperative Program managed by the Multi-disciplinary Center for Earthquake Engineering Research (MCEER). Helps during the testing from staffs and students at the Structural Laboratory and CIPRES of the Hunan University are warmly appreciated.

References

- ACI318 (1999), "Building code requirements for reinforced concrete", American Concrete Institute, Detroit.
- AIJ (1991), "Standards for structural calculation of steel reinforced concrete structures", Architectural Institute of Japan.
- AISC (1999), "Seismic provision for structural steel buildings", American Institute of Steel Construction, Chicago.
- AISC (2001), "Load and resistance factor design", Manual of Steel Construction, Third edition, American Institute of Steel Construction, Chicago.
- Anderson, C.J., Duan, J., Xiao, Y. and Maranian, P. (2002), "Cyclic testing of moment connections upgraded with weld overlays", *J. Struct. Eng.*, ASCE, **128**(4), 509-516.
- Anderson, C.J. *et al.* (1995), "Seismic behavior of HSC exterior beam-to-column connections", Department of Civil Engineering, University of Southern California.
- ASCE Task Committee (1994), "Guidelines for design of joints between steel beams and reinforced concrete columns", *J. Struct. Eng.*, ASCE, **120**(8), 2330-2357.
- Bertero, V.V., Anderson, J.C. and Krawinkler, H. (1994), "Performance of steel building structures during the Northridge earthquake", Earthquake Engineering Research Center, Report No. UCB/EERC-94-09, August.
- Bertero, V.V. *et al.* and Xiao, Y. (1995), "Seismological and engineering aspects of the January 17, 1995 Hyogoken-Nanbu (Kobe) earthquake", Earthquake Engineering Research Center, No. UCB/EERC-95/10, University of California, Berkeley, November, 250p.
- Chou, C.C. and Uang, C.M. (1998), "Experimental and analytical studies of two types of moment connections for composite special moment frames", Report No. SSRP 98-12, San Diego, La Jolla, (CA): Department of Structural Engineering, University of California, 1998.
- Chou, C.C. and Uang, C.M. (2000) "Experimental studies of composite-SMF connections with reinforced-concrete-encased column and steel beams", *Composite and Hybrid Structures – Proc. of 6th ASCCS Conf.*, Xiao and Mahin, editors, Los Angeles, March 22-24, 729-736.
- Deierlein, G.G., Sheikh, T.M., Yura, J.A. and Jirsa, J.O. (1989), "Beam-column moment connections for composite frames: Part 2", *J. Struct. Eng.*, ASCE, **115**(11), 2877-2896.
- FEMA (1994), "Recommended provisions for the development of seismic regulations for new buildings", Washington, (DC): FEMA-222A, National Earthquake Hazards Reduction Program, Building Seismic Safety Council, 1994.
- FEMA (2000), "Recommended seismic design criteria for new steel moment - frame buildings", Federal Emergency Management Agency, FEMA 350, Washington, D.C.
- Griffis, L. (1986), "Some design considerations for composite-frame structures", *AISC Eng. J.*, **23**(2), 59-64.
- Peng, S.W., Ricles, J.M., Sause, R. and Lu, L.W. (2000), "Experimental evaluation of a post-tensioned moment connection for steel and composite frames in seismic zone", *Composite and Hybrid Structures – Proc. of 6th ASCCS Conf.*, Xiao and Mahin, editors, Los Angeles, March 22-24, 721-728.

- Priestley, M.J.N., Seible, F. and Calvi, M. (1996), "Seismic design and retrofit of bridges", *Wiley Interscience*, 686p.
- Shahrooz, B.M., Deason, J.T. and Tunc, G. (2000), "Cyclic behavior of outrigger beam-wall connections", *Composite and Hybrid Structures – Proc. of 6th ASCCS Conf.*, Xiao and Mahin, editors, Los Angeles, March 22-24, 785-793.
- Sheikh, T.M., Deierlein, G.G., Yura, J.A. and Jirsa, J.O. (1989) "Beam-column moment connections for composite frames: Part 1", *J. Struct. Eng.*, ASCE, **115**(11), 2858-2876.
- Shen, Q. and Kurama, Y.C. (2000), "Lateral load behavior of unbonded post-tensioned hybrid coupled walls", *Composite and Hybrid Structures – Proc. of 6th ASCCS Conf.*, Xiao and Mahin, editors, Los Angeles, March 22-24, 793-800.
- Xiao, Y., Anderson, J.C. and Wu, Y.T. (2003), "Development of bolted end plate connections for steel reinforced concrete composite structures", *Proc. of the Advances in Structures Steel, Concrete, Composite and Aluminum*, ASSCCA 2003, Sidney, Australia, June 23-25.
- Xiao, Y., Anderson, J.C. and Yaprak, T.T. (2001), "Shear strength of steel and concrete composite columns", *Proc. of Sixth Pacific Structural Steel Conf.*, Beijing, China, October 15-17, 2001, 1171-1176.
- Xiao, Y., Priestley, M.J.N. and Seible, F. (1996), "Seismic assessment and retrofit of bridge column footings", American Concrete Institute, *ACI Struct. J.*, **93**(1), January-February, 79-94.
- Xiao, Y. and Mahin, S. edited (2000), "Composite and hybrid structures", Vol. 1 and 2, *Proc. of 6th ASCCS Int. Conf.*, Los Angeles, March 22-24, 2000, 1220p, ISBN 0-9679749-0-9.